IEEE Access
Multidisciplinary | Rapid Review | Open Access Journal

Received May 16, 2020, accepted June 3, 2020, date of publication June 5, 2020, date of current version June 29, 2020.

Digital Object Identifier 10.1109/ACCESS.2020.3000439

Power-Law Exponent Modulated Multiscale Entropy: A Complexity Measure Applied to Physiologic Time Series

WEI HAN[1,2], ZUNJING ZHANG[1], CHI TANG[1], YILI YAN[1], ERPING LUO[1], AND KANGNING XIE[1]

[1]School of Biomedical Engineering, Air Force Medical University, Xi'an 710032, China
[2]Department of Medical Engineering, 987th Hospital, Baoji 721000, China

Corresponding authors: Erping Luo (luoerping@fmmu.edu.cn) and Kangning Xie (xiekangning@fmmu.edu.cn)

This work was supported in part by the Natural Science Foundation of Shaanxi Province under Grant 2015JM3104

ABSTRACT Quantifying the complexity of physiologic time series has long attracted interest from researchers. The multiscale entropy (MSE) algorithm is a prevailing method to quantify the complexity of signals in a variety of research fields. However, the MSE method assigns increased complexity to the mixed signal of a physiologic time series added with white noise, although the mixed signal should become less complex due to the broken correlation. In addition, the MSE method needs users to visually examine its scale dependence (shape) to better characterize the complexity of a physiologic process, which is sometimes not feasible. In this paper, we proposed a new method, namely the power-law exponent modulated multiscale entropy (pMSE), as a complexity measure for physiologic time series. We tested the pMSE method on simulated data and real-world physiologic interbeat interval time series and demonstrated that it could solve the above two difficulties of the MSE method. We expect that the proposed pMSE method or its future variants could serve as a useful complement to the MSE method for the complexity analysis of physiologic time series.

INDEX TERMS Time series, multiscale entropy, complexity, power-law, self-similarity.

I. INTRODUCTION

It has attracted considerable attentions to quantify the ''complexity'' of physiologic time series in the attempt to distinguish different conditions, e.g., between the healthy and the diseased, or between the young and the elderly [1], [2]. Complexity is intuitively connected with ''meaningful structural richness'' [3], [4]. In physiologic complexity theory, healthy systems are assigned the highest complexity because they present long-range correlations and complex variability on various scales; however, diseased systems lose their complexity due to the impaired ability to adapt to adverse conditions [5]. It is also generally accepted that neither maximally random nor perfectly ordered systems possess structures (correlation between components) [6], therefore should be assigned low complexity values.

Generally, a good physiologic complexity measure should meet the following criteria: (1) it should assign higher complexity values to physiologic time series than to periodic and (2) to random time series [7], [8]; (3) it should assign higher complexity values to a physiologic time series than to its shuffled surrogate, due to broken temporal correlations [7]; (4) it should assign reduced complexity values to the physiologic time series added with white noise, which is completely random; (5) it should assign high complexity values to healthy physiologic time series and low complexity values to the diseased [1], [8], [9].

To quantify physiologic complexity, a lot of indices have been employed including various entropy-based measures, e.g., approximate entropy [10], permutation entropy [11] and sample entropy [12]. These conventional entropy-based measures, which quantify the irregularity of time series, assign the highest complexity values to white noise, therefore are not satisfactory in describing physiologic complexity.

To solve this problem, Costa *et al.* have devised a new measure, multiscale entropy (MSE), to identify complexity in physiologic systems [9], [13] by calculating sample entropy on multiple scales of the coarse-grained version

The associate editor coordinating the review of this manuscript and approving it for publication was Ting Li.

of the original times series. Moreover, several studies have been proposed to improve the MSE method. For example, Wu *et al.* have proposed the Composite MSE to decrease the high variances on large scales [14]; Wu *et al.* have proposed Modified MSE to improve precision and avoid undefined entropy values with short time series by a moving average process [15]; Shi *et al.* have extended the MSE by using higher moments (variance and skewness) in the coarse-graining process, to discern the slight differences between complex oscillations more easily [16]. The MSE and its successive methods have become prevailing methods to quantify the complexity of signals in different research fields, including biomedical [13], [17]–[21], seismic [22], traffic [23], and financial time series [24].

We will show in the following sections of this study that the MSE method is not perfection: it meets criteria (1), (2), (3) and (5) only in an *indirect* fashion; and fails to meet criterion (4). The underlying reason is that complexity values of different time series cannot be compared directly in the MSE method. This weakness is stated by Costa *et al.*, who have noted that to better characterize the physiologic processes, one needs to take into account not only the MSE values, but also their dependence on time scales (i.e., the pattern of MSE curve) by visual inspection [9]. For example, the MSE method considers some cases as low complex, where the MSE curves have an monotonical decaying pattern. Although this strategy works well for these specific cases, the pattern is often subtle for the naked eye to capture in more general scenarios (e.g., Fig. 6).

Despite these entropy-based measures (both single scale and multiple scales), another type of complexity measure is fractality testing [25], which mainly focusses on self-similarity (or long-term persistence, or system memorability) by analyzing the scaling behavior [25], [26]. Hurst exponent H is one of the most accepted metric scaling exponents.

Combining the two types of complexity measures (entropy and fractality testing), we propose a new complexity measure, which can overcome the weakness of the MSE method and can meet the five criteria mentioned above, therefore can provide a direct complexity measure for physiologic time series.

II. POWER-LAW EXPONENT MODULATED MULTISCALE ENTROPY

The power spectrum of some complex signals contains a single power-law component, i.e., the signals' power density falls with increasing frequency as $P \propto 1/f^{\beta}$, where P is the power spectral density, f is the frequency, and β is the power-law exponent [27]. β is related to Hurst exponent H as $H = (1+\beta)/2$ for stationary signals [28], [29].

The complexity distribution over β of $1/f^{\beta}$ time series is a fundamental question. Zhang has studied this question and found that the complexity distribution over β (in the range of $0 \le \beta \le 2$) presents a bell shape, reaching maxima at $\beta = 1$ (namely, the $1/f$ noise), and reaching minima at $\beta = 0$ and $\beta = 2$ [30], [31].

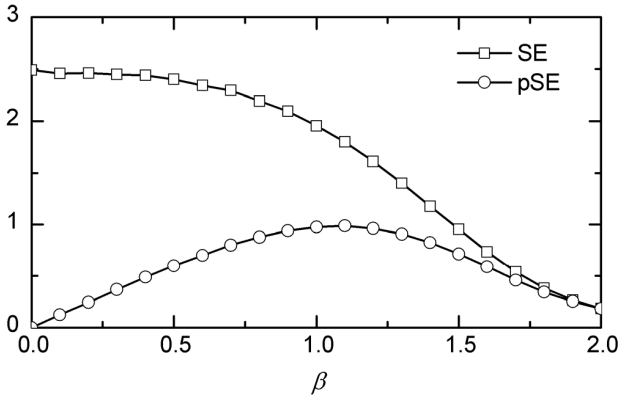

FIGURE 1. SE and pSE analysis of power-law time series with single exponent (mean: 0, variance: 1). On the *x*-axis, β is the power-law exponent. The pSE curve maximizes when β is approximately 1, which is in accordance with Zhang's complexity [30], [31].

For a power-law time series with known single power-law exponent β, we define a new complexity measure pSE as:

$$pSE = SE \cdot \frac{|\beta|}{2} \tag{1}$$

where SE is the sample entropy of the time series.

We test the pSE as a function of β of simulated power-law time series in the range of $0 \le \beta \le 2$. The result shows that the pSE curve is in accordance with the bell shape of Zhang's complexity distribution over β (Fig. 1). White noise is widely considered as having no structure and therefore possesses no complexity. Sample entropy assigns the highest value to white noise (Fig. 1 SE curve). In contrast, pSE assigns zero to white noise (Fig. 1 pSE curve).

A real-world physiologic time series usually has a spectrum of unknown power-law exponents, therefore the pSE method needs to be generalized. In order to do that, we first study the analytical formula of multiscale entropy and try to work out a way to estimate the scale-wise local power-law exponents. Then we compute pSE on each time scale by multiplying the scale-wise sample entropy and the scale-wise local power-law exponents, a method we would call power-law exponent modulated multiscale entropy (pMSE). Finally, we average pMSE over all scales to get an overall vision of the underlying complexity of the time series in question.

A. THE RELATIONSHIP BETWEEN MSE AND β

After the invention of the MSE method [13], Costa *et al.* have given the analytical formula of the MSE method in the form of a double integration (see (a-1) in Appendix) [9], which is not clear in revealing the relationship between MSE and some hidden parameters. Therefore, we further solve the double integration for $0 \le \beta < 1$ (see Appendix section for details) as follows,

$$E(s) \approx -\ln\left(\frac{r(2-\beta)}{2\sqrt{\pi(1-\beta)}}\right) + \left(\frac{\beta-1}{2}\right)\ln s \tag{2}$$

where, $E(s)$ is the multiscale entropy on scale s, the sign ln indicates the natural logarithm, and r is the tolerance factor,

a percentage of standard deviation of the time series [9]. From (2), multiscale entropy is not only related to tolerance factor r and scale factor s, which is the same as [9], but also related to an additional parameter β.

Since tolerance factor r is often a constant, and β is fixed for a given time series with single exponent, the MSE curve $E(s)$ is proportional to ln$s$ as

$$E(s) \propto \frac{\beta - 1}{2} \ln s = slope \cdot \ln s$$
$$slope \approx \frac{\beta - 1}{2} \tag{3}$$

B. ESTIMATION OF SCALE-WISE LOCAL β BASED ON THE RELATIONSHIP BETWEEN MSE AND β

From (3) we propose that, for a complex time series, the scale-wise local power-law exponents can be estimated as

$$\hat{\beta}_{scale} = 2slope_{scale} + 1 \tag{4}$$

where $slope_{scale}$ is the local slope of MSE curve on a specific scale, and $\widehat{\beta}_{scale}$ is the estimated β on that scale.

In practice, estimating the slope on each scale directly from the MSE curve may be affected by the variance of MSE. One way to address this problem is to first fit a polynomial of certain degree (e.g., fourth degree) to the MSE curve (against the natural logarithm of scales), then to differentiate the polynomial to get the local slopes and finally calculate the $\widehat{\beta}_{scale}$.

C. A MULTISCALE COMPLEXITY MEASURE: POWER-LAW EXPONENT MODULATED MULTISCALE ENTROPY

From Section II-A and II-B, we have both MSE values (i.e., sample entropy on each scale) and the $\widehat{\beta}_{scale}$. Next, we generalize the pSE to pMSE by calculating pSE on multiple time scales. We define pMSE on each scale as

$$\begin{aligned} pMSE &= SE_{scale} \cdot \frac{|\widehat{\beta}_{scale}|}{2} \\ &= SE_{scale} \cdot |slope_{scale} + 0.5| \end{aligned} \tag{5}$$

where SE_{scale} is the sample entropy on each scale.

In the conventional MSE algorithm, sample entropy calculation on coarse-grained time series uses the variance of the original time series to determine the tolerance level [13], whereas the refined MSE algorithm uses the variance of each coarse-grained time series [32]. We compare the two and find no significant difference in computing pMSE. Therefore, in (5), we simply use the conventional MSE's values on each scale for SE_{scale}.

D. AVERAGE PMSE AS A COMPLEXITY MEASURE FOR PHYSIOLOGIC TIME SERIES

We define average pMSE (apMSE) as a complexity measure of a complex physiologic time series as

$$apMSE = \frac{1}{S_H} \sum_{scale=1}^{S_H} pSE_{scale} \tag{6}$$

where S_H is the highest scale (typically 20).

For comparison, we also define average MSE (aMSE) as

$$aMSE = \frac{1}{S_H} \sum_{scale=1}^{S_H} SE_{scale} \tag{7}$$

where S_H is the same as in (6).

In summary, the algorithm takes four steps:

Step 1: Calculate the original MSE and change the linear scales to natural logarithmic ones.

Step 2: Fit a polynomial (typically of fourth degree) to the MSE curve (against the natural logarithm of scales) to get a Matlab fit object.

Step 3: Differentiate the fit object to get the local power-law exponent $\widehat{\beta}_{scale}$ (Section II-B).

Step 4: Calculate pMSE and apMSE as in (5) and (6).

The algorithm is publicly available at website https://github.com/kangningxie, with supporting codes from other research groups.

III. VALIDATION

The validation procedure of the new complexity measure pMSE is described in this section.

In the following analysis, MSE was used as a benchmark method. The MSE toolbox was kindly provided by Ahmed and Mandic [33]. The sample entropy function in the toolbox was replaced with a rapid algorithm from Pan *et al.* [34].

A. THE RELATIONSHIP BETWEEN MSE SLOPE AND POWER-LAW EXPONENT HOLDS FOR WIDER RANGE

In order to test the validity of proposed estimation method of β in Section II-B, we reconstructed the β parameters from simulated power-law time series with preset β parameters and then compared them statistically.

The power-law time series were generated with preset β from 0 to 2, and a step of 0.2. Each time series had 30000 data points. The dataset was produced by the Matlab toolbox powernoise.m provided by [35].

The scale-wise local power-law exponent $\widehat{\beta}_{scale}$ was calculated from (4) for each scale of every time series. Then, $\widehat{\beta}$ was calculated as averaged $\widehat{\beta}_{scale}$ on all scales of a specific time series. Later, $\widehat{\beta}$ was plotted against β to reveal their relationship (Fig. 2). Correlation test was then carried out between the two parameters. $\widehat{\beta}$ was a good estimator except for β values very close to 2 (correlation coefficient $R = 0.986$, $P < 0.01$). Therefore, although the relationship between MSE curve and β in (2) was theoretically established for $0 \leq \beta < 1$, it should be valid in broader range ($0 \leq \beta < 2$).

B. COMPLEXITY ANALYSIS OF SIMULATED POWER-LAW PROCESS

Although the pMSE method was proposed as a complexity measure for real-world physiologic time series with unknown β, we first validated the pMSE method on the simulated power-law time series with known β.

The power-law time series were generated with known β: 0, 0.3, 0.8, 1. Each time series had 30000 data points. MSE and pMSE were both applied to each of these time series.

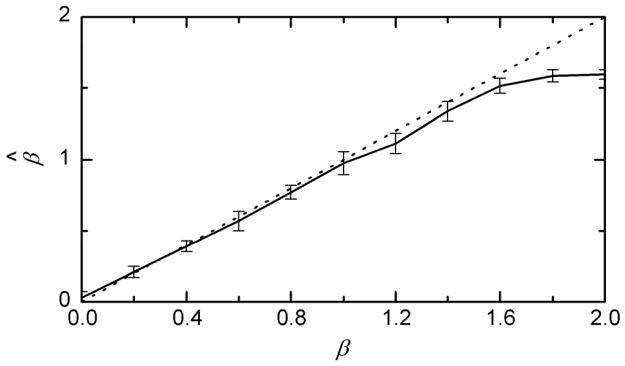

FIGURE 2. Performance analysis of the power-law exponent estimation method. $\hat{\beta}$ is the reconstructed power-law exponent from the simulated time series with given power-law exponent β. This estimation process was repeated for 30 times. The error bars show the standard deviation. For most cases of β, $\hat{\beta}$ is a good estimator (correlation coefficient $R = 0.986$, $P < 0.01$).

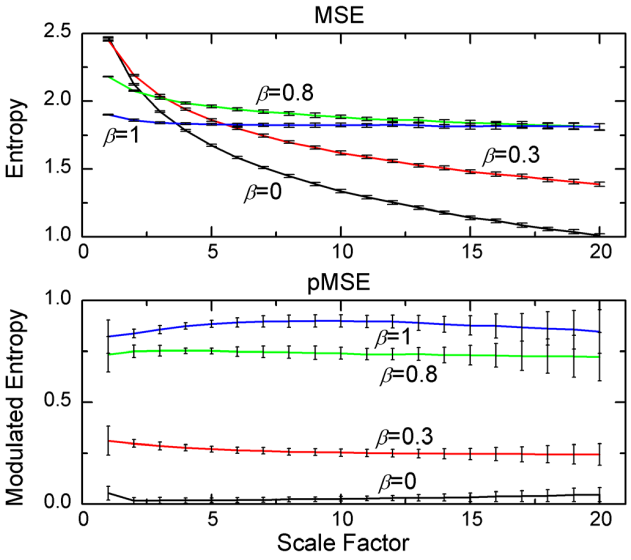

FIGURE 3. MSE (top) and pMSE (bottom) analysis of 30 simulated power-law time series, each with 30000 data points. The error bars show the standard deviation. The curve with $\beta = 0$ is the white noise, and that with $\beta = 1$ is $1/f$ noise. In the conventional MSE method, the four power-law curves are intercepted, whereas the pMSE curves show clear separation.

In Fig. 3 top, sample entropy of the white noise ($\beta = 0$) is the highest (see the scale factor 1), indicating highest irregularity other than complexity. The MSE method can indirectly indicate that white noise has low complexity by showing a declining pattern, i.e., high MSE values on small scales and low on large scales.

Determining complexity by looking at the large scales is valid for $\beta = 0$, 0.3 and 1, but it has difficulties in explaining whose complexity is higher for time series with $\beta = 0.8$ and 1 due to the fact that the MSE values of time series with $\beta = 0.8$ are all higher than those of $\beta = 1$ (Fig. 3 top). One way to settle this problem is to calculate larger scales than 20 at the cost of requirement of longer time series and higher computation load. Another way is to consider the shape.

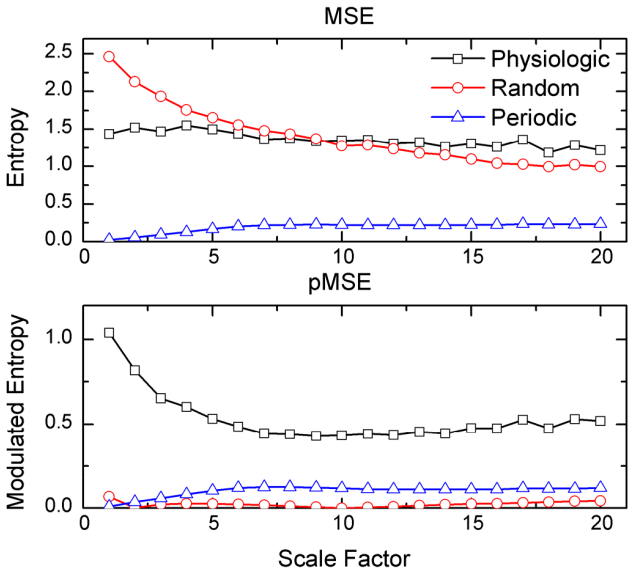

FIGURE 4. MSE (top) and pMSE (bottom) analysis of periodic, random, and physiologic series. Figure legend in bottom is the same as the one in top. pMSE directly shows higher values for physiologic time series and low values for both random and periodic time series.

The steeper decaying pattern of the MSE curve must be considered to recognize its lower complexity.

In contrast, the pMSE method consistently presents the descending complexity values to time series with β declining from 1 to 0 (Fig. 3 bottom). This result is consistent with the pSE method with known β shown in Section II.

C. COMPLEXITY ANALYSIS OF PERIODIC, RANDOM AND PHYSIOLOGIC TIME SERIES

MSE and pMSE were applied to random, periodic, and physiologic time series to compare the performance.

Periodic data was generated by a sine function $\sin(t)$, t was from 0 to 99.99 with a step of 0.01. White noise was generated as random time series. A typical interbeat interval time series was chosen as the physiologic time series, which was from Physiobank (nsrdb, 16265) [36]. Data length for each time series was 10000.

Both pMSE and MSE correctly present curves with low values for periodic time series (Fig. 4). Therefore, both methods meet criterion (1) mentioned in Introduction section.

For white noise, MSE presents a decaying pattern, very high on small scales and low on large scales (Fig. 4 top). This makes it indirect in determining the complexity level. Whereas pMSE yields a curve with low values to white noise across all scales, and relative higher curve to the physiologic time series for all scales than white noise (Fig. 4 bottom). Therefore, the pMSE method meets criterion (2) directly.

D. COMPLEXITY ANALYSIS OF PHYSIOLOGIC AND SHUFFLED TIME SERIES

MSE and pMSE were applied to a physiologic time series and its shuffled surrogate to compare the difference.

The original physiologic time series was the same as in Section III-C. The shuffled surrogate was produced by

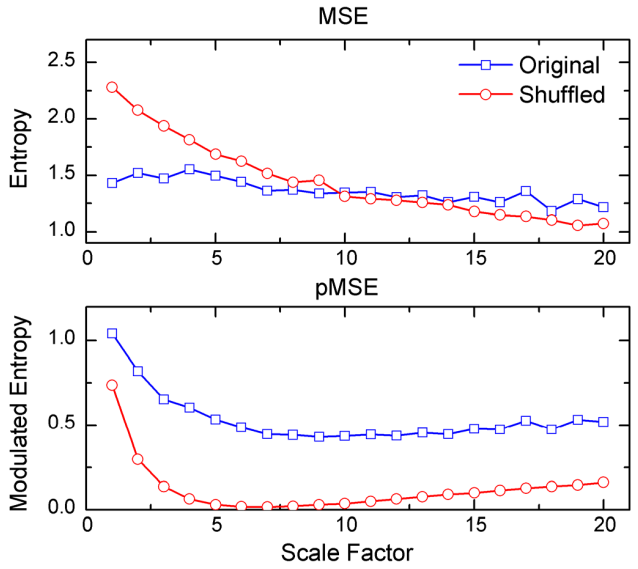

FIGURE 5. MSE (top) and pMSE (bottom) analysis of original physiologic time series and its shuffled version. Figure legend in bottom is the same as in top. pMSE straightforwardly shows clear separation of physiologic time series and its shuffled surrogate.

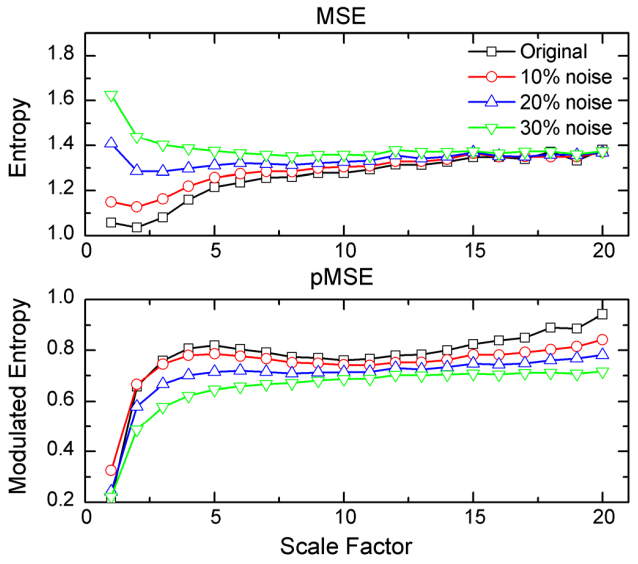

FIGURE 6. MSE (top) and pMSE (bottom) analysis of interbeat interval time series of a healthy subject, added with Gaussian white noise of increasing intensities. Figure legend in bottom is the same as in top. pMSE straightforwardly and correctly shows decreasing complexity values for mixed signals with more white noise.

shuffling the order of time sequence of the original physiologic time series. The shuffling process used the Matlab random permutation function (randperm).

In Fig. 5 top, MSE of the shuffled surrogate shows a decaying pattern. For scales smaller than 10, the shuffled MSE curve is higher than the original; for the rest of the scales, the opposite result occurs. This is a pattern similar to the MSE curve of white noise. Users of MSE are supposed to mentally regard it as lower complexity, which is neither straightforward nor quantitative. Therefore, MSE can only meets criterion (3) indirectly.

In contrast, the pMSE method show values of shuffled surrogate consistently lower than the original time series on all scales (Fig. 5 bottom). This reduced complexity can be caused by the broken correlation of time series by the shuffling. Therefore, the pMSE method can correctly and directly distinguish the complexity of a physiologic time series and its shuffled surrogate, which meets criterion (3).

E. COMPLEXITY ANALYSIS OF PHYSIOLOGIC TIME SERIES CONTAMINATED WITH WHITE NOISE

A very important aspect of a complexity measure is to report lower values to a time series contaminated with white noise. Therefore, we further tested the MSE and pMSE methods on physiologic time series with superimposed white noise of different intensities.

The physiologic time series was from a healthy subject from Physiobank (Database: MIT-BIH Normal Sinus Rhythm Database, record: 16273, length of data points: 30000) [36]. All datasets were normalized by their own standard deviations. The original time series was mixed with Gaussian white noise of different intensities, 10%, 20% and 30% standard deviation of the original time series.

The MSE method shows higher curve for mixed signals with more white noise (Fig. 6 top). For signals with obvious noise-like decaying pattern (e.g., 30% and 20% noise), the users of the MSE method need to mentally regard them as having low complexity, which is not straightforward. Moreover, for MSE curve without a decaying pattern (10% noise and original), higher values of MSE curve would be regarded as having higher complexity, which fails to meet criterion (4).

Opposite to the MSE method, the pMSE method consistently shows decreasing values of complexity for mixed signals with more white noise (Fig. 6 bottom), which meets criterion (4) straightforwardly and correctly.

F. COMPLEXITY ANALYSIS OF INTERBEAT INTERVAL TIME SERIES OF HEALTHY SUBJECTS, SUBJECTS WITH CHF AND WITH AF

Diseases may have negative effects on the complexity of a system (and the recorded time series) [37]. We compared MSE and pMSE in the application of physiologic and pathologic time series.

The interbeat interval time series were from Physiobank (Healthy: nsrdb, $n = 15$, CHF: chfdata, $n = 14$, AF: ltafdb, $n = 16$) [36]. Data length for each time series was 10000.

Different scales may represent different physiological conditions [16], [38], [39]. In the analysis of interbeat interval time series, "small" or "large" time scales are usually used when scales are shorter or longer than one typical respiratory cycle length, approximately five cardiac beats [9].

The MSE curves (Fig. 7 top) agree with the results in [9], [13]. The MSE method is successful in explaining that interbeat time series from healthy subjects have higher complexity than those from AF and CHF patients on large scales by

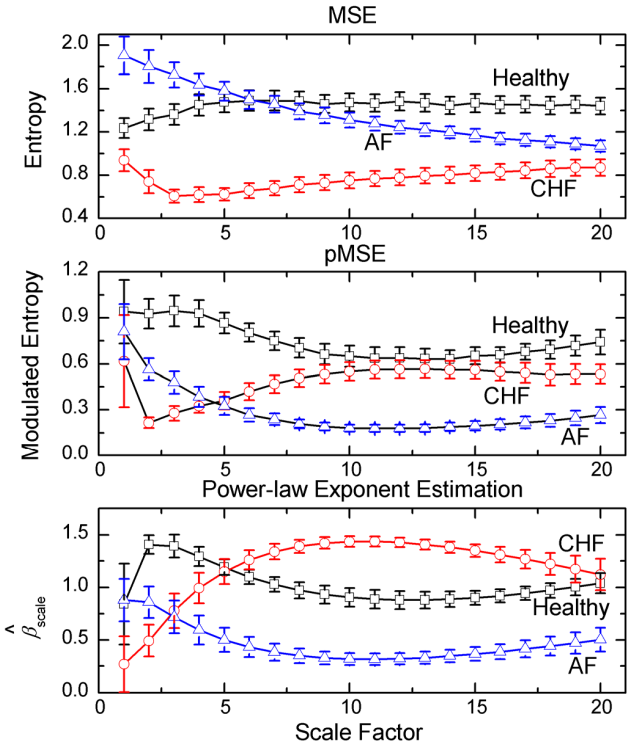

FIGURE 7. MSE (top), pMSE (middle) and estimated power-law exponent (bottom) of interbeat interval time series derived from healthy subjects ($n = 15$), subjects with congestive heart failure (CHF, $n = 14$), and subjects with atrial fibrillation (AF, $n = 16$). The error bars show the standard error. For most scales, the descending order of pMSE curves is: Healthy, CHF, AF, which is more straightforward than MSE.

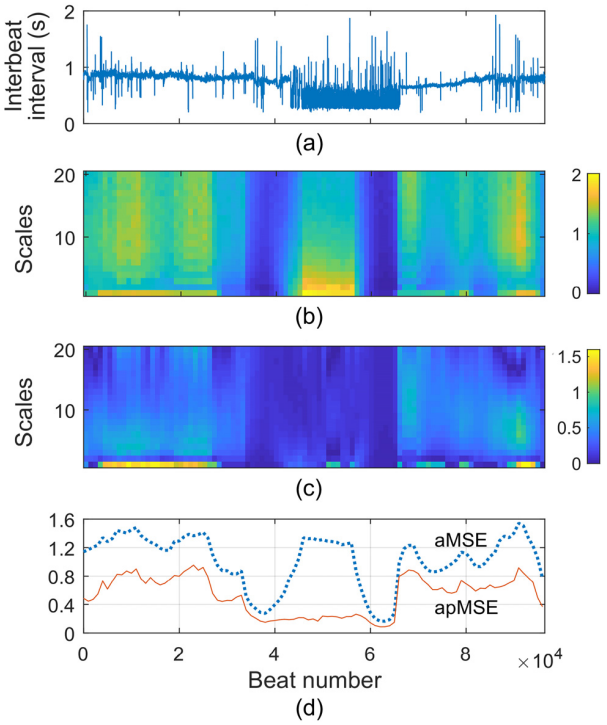

FIGURE 8. Sliding window analysis of a long time series from subjects with paroxysmal atrial fibrillation. (a): Interbeat interval (second) over beat numbers. (b) and (c): MSE and pMSE over beat numbers using sliding window method. (d): the average MSE (aMSE) and average pMSE (apMSE) over beat numbers. apMSE drops during onset of AF (40000-60000), presenting a good complexity indicator.

considering the values only; yet, it has difficulties in explaining that time series from AF patients have less complexity than that from CHF patients and healthy subjects. This has been the reason to take into account the shape of MSE curves [9]. One can recognize the low complexity nature of AF time series from its monotonic decaying pattern of MSE, which is similar to that of white noise. Overall, the MSE method meets criterion (5) indirectly.

In contrast, on large scales, the pMSE method shows consistent highest values for healthy subjects, and lowest values for AF subjects (Fig. 7 middle). One does not need to further examine the shape of pMSE curves to assign complexity levels to the three time series. The pMSE method directly shows higher complexity to physiologic time series than to pathologic time series. Therefore, pMSE meets criterion (5) directly.

In addition, Fig. 7 middle shows that, for the two pathologic time series, there is an interception of curves from CHF and AF at time scale 5. On large scales, pMSE curve from CHF is higher than that from AF. However, on small scales, pMSE curve from AF is higher than that from CHF. This result suggests that the underlying controlling processes from the two diseased cases may be differently affected by respiration.

In addition, we estimated $\widehat{\beta}$ on each scale (i.e., $\widehat{\beta}_{scale}$) from the MSE curve by (4) (Fig.7 bottom). Interestingly, the $\widehat{\beta}$ values present some similarities to the slope of detrended fluctuation analysis (DFA) of both healthy subjects and subjects with CHF [40]. For example, the $\widehat{\beta}$ values from healthy subjects are high (peak value is about 1.5) on low scales, decaying to 1 on higher scales; the $\widehat{\beta}$ values from CHF subjects are low on small scales and high on large scales.

G. COMPLEXITY ANALYSIS OF LONG-TERM PAROXYSMAL AF INTERBEAT INTERVAL TIME SERIES

A long-term paroxysmal AF interbeat interval time series was used to compare aMSE and apMSE.

The time series was from Physiobank database: ltafdb, record:00 [36]. The calculation was on sliding windows (window size: 10000; overlap: 9000, sliding step: 1000). MSE (Fig. 8 b) and pMSE (Fig. 8 c) vs. beat numbers of a long-term paroxysmal AF interbeat interval time series (Fig. 8 a). aMSE and apMSE were computed on sliding windows (Fig. 8 d).

We observe that: 1) the MSE and pMSE can both be plotted over beat number in sliding windows to show time-varing features, with some similarities to time-frequency analysis of a signal; 2) overall, aMSE and apMSE have similar trend during time course without AF; 3) during the time course of AF, aMSE still presents the same level (except for short time periods just before and after the AF), whereas the apMSE curve consitently drops, indicating that AF has low complexity. Therefore, apMSE may serve as an applicable single-valued indicator of complexity.

IV. DISCUSSION

Determining the complexity of power-law time series is a funamental problem, which has been addressed by Zhang [30] that the complexity of power-law time series peaks when power-law exponent is 1 ($1/f$ noise) and declines when it goes either up or down, reaching minima at 0 and 2. In accordance with Zhang's finding, Costa *et al.* [9] also show $1/f$ (power-law exponent $\beta = 1$) noise has high complexity and white noise (power-law exponent $\beta = 0$) has low complexity in their proposed MSE method.

Despite these separate cases, Costa *et al.* have not shown broader cases with continuous power-law exponents. In addition, MSE will give a fundamental misleading result when a complex time series is added with white noise: MSE shows higher curves indicating higher complexity while less complexity should be reported due to the contamination of structure by the white noise (Fig. 6), as stated in criterion (5). Another difficulty of MSE is that it relies on users to mentally identify a decaying pattern to rule out ''noise-like'' pattern instead of quantitively assigning a complexity number (AF case in Fig. 7), therefore it is not a direct measure of complexity in criteria (1), (2), (3) and (5).

In this study, we have demonstated that pSE of power-law time series has the same distribution pattern over power-law exponent from 0 to 2 as that in Zhang's study. Also, we have given the detailed analytical formula for conventional MSE of power-law time series with power-law exponent β. The results have shown that, when the scale factor is in natural logarithm, the slope of MSE curve is directly proportional to the power-law exponent β (Appendix (a-10)). This relationship is valid for β in the range of $0 \leq \beta < 2$ (Fig. 2).

We notice that Gao *et al.* [41] has given the same results in terms of the relationship between the slope of MSE and Hurst exponent, which is equivalent to our findings when β is in the range of $0 \leq \beta \leq 1$. In addition, in the range of $1 < \beta < 2$, our proposed relationship still holds, suggesting that the power-law exponent might be a more fundamental parameter than Hurst parameter. Therefore, we can estimate the local β from the MSE curve and calculate the local pSE as a complexity measure on the specific scale, a method we call the power-law exponent modulated multiscale entropy (pMSE).

The proposed pMSE assigns high complexity values to physiologic time series and low complexity values to both periodic and random time series (the first and second criteria). Furthermore, pMSE correctly presents a consistently higher curve to a physiologic time series than to its shuffled surrogate (the third criterion). pMSE correctly assigns lower values to physiologic time series contaminated with white noise (the fourth criterion). For the comparison of healthy and pathologic time series, pMSE presents a straightforward way to show the complexity levels, which meets criterion (5).

For the comparison of pMSE and MSE, all parameters that calculate MSE are selected the same as in [13]. The degree of polynomial that fits the MSE curve affects the performance of pMSE. Generally, higher degree tends to overfit the curve and lower degree might not be adequate to capture the pattern. Although no detailed analysis is shown in this paper, we would empirically suggest the fourth degree be a reasonable choice.

We note that Silva *et al.* have proposed generalized sample entropy based on Tsallis nonadditive statistics and defined a complexity measure as the difference of this generalized sample entropy on one signal and its surrogate [7]. Silva's complexity measure can also satisfy the criteria mentioned in Introduction section, yet the computation cost is high (It needs to compute the generalized sample entropy for 100 surrogate series).

Our pMSE method may be improved benefitting from the techniques introduced in the successive MSE methods (for a review, see [42]), some of which aim to improve the estimation accuracy, and some to optimize the coarse-graining procedure. However, pMSE may have difficulties in directly benefitting from the multiscale permutation entropy (MPE) [43], due to the major difference between sample entropy and permutation entropy, which extracts a probability distribution of the ordinal patterns.

V. CONCLUSION

We have proposed and tested a new physiologic complexity measure (pMSE) to characterize the complexity of physiologic time series. The pMSE overcomes the weakness of the MSE method (complexity values of different time series cannot be compared directly) and meets all five criteria mentioned in Introduction section, therefore may provide a promising complexity measure for physiologic time series.

APPENDIX

First, for uncorrelated Gaussian noise, one can observe n data points, $x_1, x_2, \cdots, x_n$. Consider that each data point comes from uncorrelated stochastic variables X. Costa, *et al.* [9] calculated the sample entropy,

$$SE = -\ln P_r(|x_j - x_i| \leq r\sigma)$$

where P_r is the probability that the distance between two data points of the coarse-grained time series (with scale s) is less than or equal to a predefined threshold r. Note that, the original equation in [9] is $SE = -\ln P_r(|x_j - x_i| \leq r)$, which is correct when the time series has standard deviation $\sigma = 1$, otherwise the equation $SE = -\ln P_r(|x_j - x_i| \leq r\sigma)$ should be used.

This probability was shown as the following double-integral form

$$P_r(|x_j^s - x_i^s| \leq r\sigma) = \frac{\sqrt{s}}{2\sigma}\sqrt{\frac{1}{2\pi}}\int_{-\infty}^{\infty}\left\{\mathrm{erf}\left(\frac{x+r}{\sigma\sqrt{2/s}}\right) - \mathrm{erf}\left(\frac{x-r}{\sigma\sqrt{2/s}}\right)\right\}e^{-x^2 s/2\sigma^2}dx \tag{a-1}$$

where erf refers to the error function:

$$\mathrm{erf}(x) = \frac{2}{\sqrt{\pi}} \int_0^x e^{-u^2} du$$

and σ is the standard deviation of the original time series of scale 1. The threshold r is often chosen as a constant in the range of 0.15-0.3.

Next, Costa derived the analytical MSE for $1/f$ noise by mapping the correlated noises into white noises via orthogonal transformation. The correlated noise is assumed to come from a fractal Gaussian noise (fGn) process. It has a time-independent autocorrelation function depending only on lag and Hurst exponent [28]. Let us consider n random variables $X_i (i = 1, 2, \cdots n)$. There is an orthogonal transform matrix U^T (formed with eigenvectors U_i of the covariance matrix of X_i) which can transform correlated X_i into uncorrelated (independent) Y_i with Gaussian distribution with standard deviation of $\sigma_{Y_i} = \sqrt{\lambda_i}$, where λ_i is the Eigen values corresponding to the U_i.

Now we have n uncorrelated Gaussian variable Y_i with an average standard deviation of $\bar{\sigma}_Y = \frac{1}{n}\sum_i^n (\sigma_{Yi}) = \frac{1}{n}\sum_i^n (\sqrt{\lambda_i})$. For each coarse-grained sequence with scale s, the data length becomes $\frac{n}{s}$. Therefore, the average standard deviation of the coarse-grained sequence becomes

$$\bar{\sigma}_{Ys} = \frac{s}{n}\sum_i^{n/s} (\sigma_{Yi}) = \frac{s}{n}\sum_i^{n/s} (\sqrt{\lambda_i}) \tag{a-2}$$

Li proved that when the sampling data length n is sufficiently large, the eigenvalues of a fractal Brownian motion (fBm) process with Hurst exponent H decays as a power-law [44]

$$\lambda_i \approx \frac{K}{i^{2H+1}} \tag{a-3}$$

where K is a constant related to H.

The power versus frequency relationship of fBm process is $|A(f)|^2 \propto c_0 \cdot f^{-\beta}$, where β is the power-law exponent. The Hurst exponent H is related with β when $\beta > 1$ [28]: $H = (\beta - 1)/2$, therefore, (a-3) becomes

$$\lambda_i \approx \frac{K}{i^{\beta}} \tag{a-4}$$

Although this is derived from fBm process, we expect that it is also valid for fGn process without proof. Since the transform of X to Y does not change the energy, we have

$$n\sigma_X^2 = n\sigma_Y^2 \approx \sum_{i=1}^{n} \frac{K}{i^{\beta}}$$

The right-hand side of the above equation can be estimated by the partial sum of p-series [45]

$$\sum_{i=1}^{n} \frac{K}{i^{\beta}} \approx \frac{Kn^{1-\beta}}{1-\beta}$$

Combine the above two equations, we have $K = \sigma_X^2(1-\beta)n^{\beta}$

Equation (a-4) becomes $\lambda_i \approx \frac{K}{i^{\beta}} = \frac{\sigma_X^2(1-\beta)n^{\beta}}{i^{\beta}}$

The mean standard deviation of scaled and transformed time series is

$$\begin{aligned}\bar{\sigma}_{Ys} &= \frac{1}{n/s}\sum_{i=1}^{n/s} \sqrt{\lambda_i} \\ &\approx \frac{1}{n/s}\sum_{i=1}^{n/s} \left(\frac{\sigma_X^2(1-\beta)n^{\beta}}{i^{\beta}}\right)^{1/2} \\ &= \frac{2s^{\beta/2}\sigma_X\sqrt{1-\beta}}{2-\beta}\end{aligned} \tag{a-5}$$

The multiscale entropy of scale factor s can now be calculated on the Gaussian distribution of mean zero and standard deviation $\bar{\sigma}_{Ys}$ by the following equation

$$E(s) = -\ln(P_r(|y_j^s - y_i^s| \le r\sigma_X)) = -\ln(\mathrm{erf}(\frac{\sqrt{s}r\sigma_X}{2\bar{\sigma}_{YS}})) \tag{a-6}$$

The erf function can be written as the Taylor series, and for typical settings, $\frac{\sqrt{s}r\sigma_X}{2\bar{\sigma}_{YS}} < 1$. Therefore,

$$\mathrm{erf}(x) = \frac{2}{\sqrt{\pi}}(x - \frac{x^3}{3} + \frac{x^5}{10} + \mathrm{L})$$

Apply the first order expansion of erf(x), we have

$$\mathrm{erf}(\frac{\sqrt{s}r\sigma_X}{2\bar{\sigma}_Y}) \approx \frac{2}{\sqrt{\pi}}\frac{\sqrt{s}r\sigma_X}{2\bar{\sigma}_{YS}}$$

Therefore,

$$E(s) = -\ln(P_r(|y_j^s - y_i^s| \le r\sigma_X)) \approx -\ln(\frac{2}{\sqrt{\pi}}\frac{\sqrt{s}r\sigma_X}{2\bar{\sigma}_{YS}}) \tag{a-7}$$

According to (a-5) and (a-7), we finally have the analytical formula for MSE:

$$\begin{aligned}E(s) &= -\ln(P_r(|y_j^s - y_i^s| \le r\sigma_X)) \\ &\approx -\ln(\frac{r(2-\beta)}{2\sqrt{\pi(1-\beta)}}) + (\frac{\beta-1}{2})\ln s\end{aligned} \tag{a-8}$$

where, $0 < \beta < 1$ and $E(1)$ is the entropy at scale 1.

In Fig. 9, the analytical and numerical MSE values are plotted against the natural logarithms of scale factors, from ln1 to ln20. The power-law exponents β are set from 0.1 to 0.9 with step 0.1. We observe that the analytical (a-8) and numerical MSE curves are similar for different β values, and the small goodness of fit values (defined as the normalized root mean square error: 0.0033195) showed that the analytical and numerical MSE fit well in the range of $0 \le \beta < 0.9$.

Form (a-8), we can see that the MSE curve $E(s)$ of time series with power-law exponent β is proportional to ln$s$ and ln$r$. In practice, r is often fixed, and (a-8) can be reduced to

$$E(s) \propto \frac{\beta-1}{2}\ln s = slope \cdot \ln s \tag{a-9}$$

where

$$slope = \frac{\beta-1}{2} \tag{a-10}$$

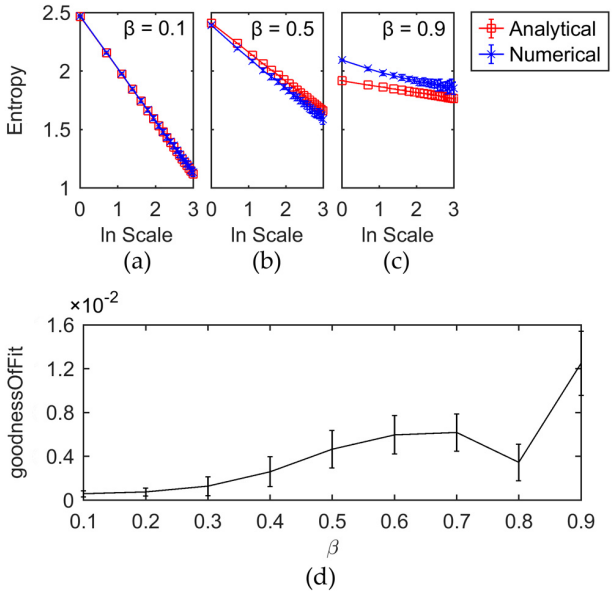

FIGURE 9. Analytical and numerical entropy comparison while $0 < \beta < 1$ and $r = 0.15$. (a-c) shows the MSE against the natural logarithms of scale factor of three simulated power-law time series with $\beta = 0.1$, 0.5, and 0.9, respectively. (d) shows the goodness of fit of analytical entropy to the numerical entropy as a function of β.

For the estimation of this relation between MSE slope and β, see Section V-A.

ACKNOWLEDGMENT

(Wei Han and Zunjing Zhang contributed equally to this work.)

REFERENCES

[1] S. M. Pincus, "Assessing serial irregularity and its implications for health," *Ann. New York Acad. Sci.*, vol. 954, pp. 245–267, Dec. 2001.

[2] H. X. Zhang, Y. S. Zhu, and Z. M. Wang, "Complexity measure and complexity rate information based detection of ventricular tachycardia and fibrillation," *Med. Biol. Eng. Comput.*, vol. 38, no. 5, pp. 553–557, Sep. 2000.

[3] P. Grassberger, *Information Dynamics*. New York, NY, USA: Plenum, 1991.

[4] D. P. Feldman and J. P. Crutchfield, "Measures of statistical complexity: Why?" *Phys. Lett. A*, vol. 238, nos. 4–5, pp. 244–252, Feb. 1998.

[5] A. L. Goldberger, C.-K. Peng, and L. A. Lipsitz, "What is physiologic complexity and how does it change with aging and disease?" *Neurobiol. Aging*, vol. 23, no. 1, pp. 23–26, Jan. 2002.

[6] B.-Y. Yaneer, *Dynamics of Complex Systems*. Reading, MA, USA: Addison-Wesley, 1997.

[7] L. E. V. Silva, B. C. T. Cabella, U. P. D. C. Neves, and L. O. M. Junior, "Multiscale entropy-based methods for heart rate variability complexity analysis," *Phys. A, Stat. Mech. Appl.*, vol. 422, pp. 143–152, Mar. 2015.

[8] A. L. Goldberger, L. A. Amaral, J. M. Hausdorff, P. Ivanov, C. K. Peng, and H. E. Stanley, "Fractal dynamics in physiology: Alterations with disease and aging," *Proc. Nat. Acad. Sci. USA*, vol. 99, no. 1, pp. 2466–2472, Feb. 2002.

[9] M. Costa, A. L. Goldberger, and C.-K. Peng, "Multiscale entropy analysis of biological signals," *Phys. Rev. E, Stat. Phys. Plasmas Fluids Relat. Interdiscip. Top.*, vol. 71, no. 2, Feb. 2005, Art. no. 021906.

[10] S. M. Pincus, "Approximate entropy as a measure of system complexity," *Proc. Nat. Acad. Sci. USA*, vol. 88, no. 6, pp. 2297–2301, Mar. 1991.

[11] C. Bandt and B. Pompe, "Permutation entropy: A natural complexity measure for time series," *Phys. Rev. Lett.*, vol. 88, no. 17, Apr. 2002, Art. no. 174102.

[12] J. S. Richman and J. R. Moorman, "Physiological time-series analysis using approximate entropy and sample entropy," *Amer. J. Physiol.-Heart Circulatory Physiol.*, vol. 278, no. 6, pp. H2039–H2049, Jun. 2000.

[13] M. Costa, A. L. Goldberger, and C.-K. Peng, "Multiscale entropy analysis of complex physiologic time series," *Phys. Rev. Lett.*, vol. 89, no. 6, Jul. 2002, Art. no. 068102.

[14] S.-D. Wu, C.-W. Wu, S.-G. Lin, C.-C. Wang, and K.-Y. Lee, "Time series analysis using composite multiscale entropy," *Entropy*, vol. 15, no. 3, pp. 1069–1084, Mar. 2013.

[15] S.-D. Wu, C.-W. Wu, K.-Y. Lee, and S.-G. Lin, "Modified multiscale entropy for short-term time series analysis," *Phys. A, Stat. Mech. Appl.*, vol. 392, no. 23, pp. 5865–5873, Dec. 2013.

[16] W. Shi, P. Shang, Y. Ma, S. Sun, and C.-H. Yeh, "A comparison study on stages of sleep: Quantifying multiscale complexity using higher moments on coarse-graining," *Commun. Nonlinear Sci. Numer. Simul.*, vol. 44, pp. 292–303, Mar. 2017.

[17] F. Liao, G. Cheing, W. Ren, S. Jain, and Y.-K. Jan, "Application of multiscale entropy in assessing plantar skin blood flow dynamics in diabetics with peripheral neuropathy," *Entropy*, vol. 20, no. 2, p. 127, Feb. 2018.

[18] R. Okazaki, T. Takahashi, K. Ueno, K. Takahashi, M. Ishitobi, M. Kikuchi, M. Higashima, and Y. Wada, "Changes in EEG complexity with electroconvulsive therapy in a patient with autism spectrum disorders: A multiscale entropy approach," *Frontiers Hum. Neurosci.*, vol. 9, p. 106, Feb. 2015.

[19] X. Chen, Q. Guo, and D. G. Brockway, "Analyzing the complexity of cone production in longleaf pine by multiscale entropy," *J. Sustain. Forestry*, vol. 35, no. 2, pp. 172–182, Feb. 2016.

[20] Y. Wu, Y. Chen, Y. Ye, T. Yan, and R. Song, "Age-related differences in complexity during handgrip control using multiscale entropy," *IEEE Access*, vol. 6, pp. 45552–45561, 2018.

[21] P. Huang, Z. Huang, X. Lu, Y. Cao, J. Yu, D. Hou, and G. Zhang, "Study on glycoprotein terahertz time-domain spectroscopy based on composite multiscale entropy feature extraction method," *Spectrochimica Acta A, Mol. Biomole. Spectrosc.*, vol. 229, Mar. 2020, Art. no. 117948.

[22] L. Guzmán-Vargas, A. Ramírez-Rojas, and F. Angulo-Brown, "Multiscale entropy analysis of electroseismic time series," *Natural Hazards Earth Syst. Sci.*, vol. 8, no. 4, pp. 855–860, Aug. 2008.

[23] Y. Yin and P. Shang, "Multivariate multiscale sample entropy of traffic time series," *Nonlinear Dyn.*, vol. 86, no. 1, pp. 479–488, Oct. 2016.

[24] H. Niu and J. Wang, "Quantifying complexity of financial short-term time series by composite multiscale entropy measure," *Commun. Nonlinear Sci. Numer. Simul.*, vol. 22, nos. 1–3, pp. 375–382, May 2015.

[25] L. Tang, H. Lv, F. Yang, and L. Yu, "Complexity testing techniques for time series data: A comprehensive literature review," *Chaos, Solitons Fractals*, vol. 81, pp. 117–135, Dec. 2015.

[26] J. T. Barkoulas and C. F. Baum, "Long-term dependence in stock returns," *Econ. Lett.*, vol. 53, no. 3, pp. 253–259, Dec. 1996.

[27] B. J. He, "Scale-free brain activity: Past, present, and future," *Trends Cognit Sci.*, vol. 18, no. 9, pp. 480–487, Sep. 2014.

[28] A. Eke, P. Herman, J. B. Bassingthwaighte, G. M. Raymond, D. B. Percival, M. Cannon, I. Balla, and C. Ikrenyi, "Physiological time series: Distinguishing fractal noises from motions," *Pflügers Archiv., Eur. J. Physiol.*, vol. 439, no. 4, pp. 403–415, Feb. 2000.

[29] H. E. Hurst, "Long-term storage capacity of reservoirs," *Trans. Amer. Soc. Civil Eng.*, vol. 116, pp. 770–808, 1951.

[30] Y.-C. Zhang, "Complexity and 1/f noise. A phase space approach," *J. de Phys. I*, vol. 1, no. 7, pp. 971–977, Jul. 1991.

[31] X. S. Zhang, R. J. Roy, and E. W. Jensen, "EEG complexity as a measure of depth of anesthesia for patients," *IEEE Trans. Biomed. Eng.*, vol. 48, no. 12, pp. 1424–1433, Dec. 2001.

[32] J. F. Valencia, A. Porta, M. Vallverdu, F. Claria, R. Baranowski, E. Orlowska-Baranowska, and P. Caminal, "Refined multiscale entropy: Application to 24-h Holter recordings of heart period variability in healthy and aortic stenosis subjects," *IEEE Trans. Biomed. Eng.*, vol. 56, no. 9, pp. 2202–2213, Sep. 2009.

[33] M. U. Ahmed and D. P. Mandic, "Multivariate multiscale entropy: A tool for complexity analysis of multichannel data," *Phys. Rev. E, Stat. Phys. Plasmas Fluids Relat. Interdiscip. Top.*, vol. 84, no. 6, Dec. 2011, Art. no. 061918.

[34] Y. H. Pan, Y. H. Wang, S. F. Liang, and K. T. Lee, "Fast computation of sample entropy and approximate entropy in biomedicine," *Comput. Methods Programs Biomed.*, vol. 104, no. 3, pp. 382–396, Dec. 2011.

[35] M. A. Little, P. E. McSharry, S. J. Roberts, D. A. Costello, and I. M. Moroz, "Exploiting nonlinear recurrence and fractal scaling properties for voice disorder detection," *Biomed. Eng. OnLine*, vol. 6, no. 1, p. 23, 2007.
[36] A. L. Goldberger, L. A. N. Amaral, L. Glass, J. M. Hausdorff, P. C. Ivanov, R. G. Mark, J. E. Mietus, G. B. Moody, C.-K. Peng, and H. E. Stanley, "PhysioBank, PhysioToolkit, and PhysioNet: Components of a new research resource for complex physiologic signals," *Circulation*, vol. 101, no. 23, pp. 215–220, Jun. 2000.
[37] L. A. Lipsitz and A. L. Goldberger, "Loss of 'complexity' and aging. Potential applications of fractals and chaos theory to senescence," *J. Amer. Med. Assoc.*, vol. 267, no. 13, pp. 1806–1809, Apr. 1992.
[38] Y.-H. Lin, H.-C. Huang, Y.-C. Chang, C. Lin, M.-T. Lo, L.-Y.-D. Liu, P.-R. Tsai, Y.-S. Chen, W.-J. Ko, Y.-L. Ho, M.-F. Chen, C.-K. Peng, and T. G. Buchman, "Multi-scale symbolic entropy analysis provides prognostic prediction in patients receiving extracorporeal life support," *Crit. Care*, vol. 18, no. 5, Oct. 2014, Art. no. 548.
[39] V. Miskovic, K. J. MacDonald, L. J. Rhodes, and K. A. Cote, "Changes in EEG multiscale entropy and power-law frequency scaling during the human sleep cycle," *Hum. Brain Mapping*, vol. 40, no. 2, pp. 538–551, Feb. 2019.
[40] C. K. Peng, S. Havlin, H. E. Stanley, and A. L. Goldberger, "Quantification of scaling exponents and crossover phenomena in nonstationary heartbeat time series," *Chaos*, vol. 5, no. 1, pp. 82–87, 1995.
[41] J. Gao, J. Hu, F. Liu, and Y. Cao, "Multiscale entropy analysis of biological signals: A fundamental bi-scaling law," *Frontiers Comput. Neurosci.*, vol. 9, p. 64, Jun. 2015.
[42] A. Humeau-Heurtier, "The multiscale entropy algorithm and its variants: A review," *Entropy*, vol. 17, no. 5, pp. 3110–3123, May 2015.
[43] G. Ouyang, J. Li, X. Liu, and X. Li, "Dynamic characteristics of absence EEG recordings with multiscale permutation entropy analysis," *Epilepsy Res.*, vol. 104, no. 3, pp. 246–252, May 2013.
[44] L. Li, J. Hu, Y. Chen, and Y. Zhang, "PCA based hurst exponent estimator for fBm signals under disturbances," *IEEE Trans. Signal Process.*, vol. 57, no. 7, pp. 2840–2846, Jul. 2009.
[45] S. K. Goel and D. M. Rodriguez, "A note on evaluating limits using Riemann sums," *Math. Mag.*, vol. 60, no. 4, pp. 225–228, Oct. 1987.

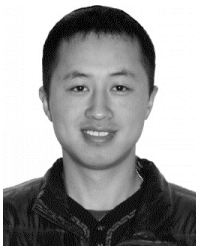

WEI HAN was born in 1990. He received the B.S. degree in biomedical engineering from Air Force Medical University, Xi'an, China, in 2012, where he is currently pursuing the M.S. degree with the School of Biomedical Engineering.

From 2013 to 2017, he was a Medical Equipment Engineer with the 987th Hospital of PLA. His current research interests include biomedical signal processing and neuroscience. Since 2018, he has been a Student Member of the Shaanxi Signal Processing Association.

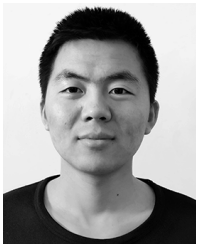

ZUNJING ZHANG was born in 1997. He received the B.S. degree in biomedical engineering from Air Force Medical University, Xi'an, China, in 2019.

His current research interests include biomedical signal processing and medical equipment.

CHI TANG was born in China, in 1977. He received the B.S., M.S., and Ph.D. degrees in biomedical engineering from Fourth Military Medical University, Xi'an, China, in 2000, 2005, and 2008, respectively.

He is currently an Associate Professor with the School of Biomedical Engineering, Air Force Medical University. His current research interests include signal processing, hypoxia injury and protective mechanism in plateau, research and development of anti-hypoxia medical equipment, and applied research of medical metrology.

YILI YAN received the B.S. and M.S. degrees in biomedical engineering from The Fourth Military Medical University, Xi'an, China. He is currently a Lecturer with the School of Biomedical Engineering, Air Force Medical University. His research interests include neural encoding, neural engineering, and signal processing.

ERPING LUO was born in Chengdu, China, in 1959. He received the Ph.D. degree in electronics science and technology from Xidian University, Xi'an, China, in 2005.

He is currently a Professor with the School of Biomedical Engineering, Air Force Medical University. His current research interests include signal processing and research and development of anti-hypoxia medical equipment.

Dr. Luo was a recipient of the Special Government Allowance and the Second Prize for National Scientific and Technological Progress. He is the Vice President of the China Medical Gases Industry Association.

KANGNING XIE was born in Jiangsu, China, in 1976. He received the B.S. degree in biomedical engineering from Fourth Military Medical University, Xi'an, China, in 1999, and the Ph.D. degree from Tsinghua University, Beijing, China, in 2013.

From 2004 to 2005, he was an Academic Visitor with the University of Oxford, U.K. He is currently an Associate Professor and the Vice Dean of the School of Biomedical Engineering, Air Force Medical University, Xi'an. His research interests include signal processing, nonlinear dynamics, and medical equipment. He is also a Committee Member of the Shaanxi Signal Processing Association.